CHAPTER - III

GYRO RESONANT INTERACTION OF WHISTLER MODE WAVE PACKETS: EXTENSION OF DAS'S MODEL FOR VLF EMISSIONS

3.1 INTRODUCTION:

In the last chapter we discussed the effect of the Landau resonance of the off angle whistler pulses with the electrons in a homogeneous collisionless magnetoplasma. It has already been pointed out earlier that a study of the wave particle interactions is likely to give clues regarding the generation mechanism of the VLF emissions. Therefore, it would be worthwhile to look into the effects caused by other resonances, too.

One of the very important resonances is gyro resonance or cyclotron resonance which occurs when the rate of change of the angle between the rotating wave vector and the velocity vector of the gyrating electron becomes zero. According to linear theory the particle should be accelerated or decelerated indefinitely during

a resonant interaction but, in practice, the change in the velocity soon upsets the resonance condition and thus brings the interaction into nonlinear regime.

For off angle whistlers the resonance condition can be mathematically put as

$$\omega - k_{\parallel} v_{\parallel} = N\Omega \quad , \quad N = 0, \pm 1, \pm 2$$

For parallel propagation (i.e. $\theta = 0$), only resonance is the gyroresonance given by

$$\omega - k_{\parallel} v_{\parallel} = \Omega$$

The relative importance of the Landau and the gyro resonances can be assessed by substituting their respective conditions in equations (2.2a) and (2.2b) and then comparing the effects produced by the two.

The rigorous treatment for this is rather involved and therefore here we attempt to have a less rigorous but simpler and more intuitive approach.

Although, both the parallel and the perpendicular components of the wavefields contribute to velocity changes during either type of resonance, the Landau resonance effects are caused mainly by the parallel

component of the wave field while the contribution to the cyclotron resonant effects comes primarily from the perpendicular wave fields. This indicates that a comparison of the parallel and the perpendicular components of the wave fields should provide a good measure of the relative importance of the two resonances and should also tell under what conditions one resonance would dominate over the other.

The dispersion relation for a wave propagating at an angle θ to a uniform magnetic field Bo embedded in a cold uniform plasma is given by an equation in which zero is equated to the determinant of the matrix on the L.H.S of the following equation (Stix, 1962)

$$\begin{bmatrix} S - n^2\cos^2\theta & -iD & n^2 \sin\theta\cos\theta \\ iD & S - n^2 & 0 \\ n^2 \sin\theta\cos\theta & 0 & P - n^2\sin^2\theta \end{bmatrix} \begin{bmatrix} E_x \\ E_y \\ E_z \end{bmatrix} = \begin{bmatrix} 0 \\ 0 \\ 0 \end{bmatrix} \quad \ldots(3.1)$$

where

$$S = \frac{1}{2}(R+L) \quad , \quad D = \frac{1}{2}(R-L)$$

$$R = 1 - \frac{\omega_p^2}{\omega^2}\left(\frac{\omega}{\omega-\Omega}\right)$$

$$L = 1 - \frac{\omega_p^2}{\omega^2}\left(\frac{\omega}{\omega+\Omega}\right)$$

$$P = 1 - \frac{\omega_p^2}{\omega^2}$$

$\vec{n} = \frac{c\vec{k}}{\omega}$ = refractive index of the medium for whistler mode waves.

and $\omega_p = \frac{4\pi n e^2}{m}$ = the electron plasma frequency

The equations (3.1) readily give,

$$\left.\begin{aligned} E_x &= C_{xz} E_z \\ \text{and} \quad E_y &= i C_{yz} E_z \\ \text{where,} \quad C_{xz} &= \frac{n^2 \sin^2\theta - P}{n^2 \sin\theta\cos\theta} \\ \text{and} \quad C_{yz} &= \frac{D}{n^2 - S} C_{xz} \end{aligned}\right\} \quad \text{---(3.2)}$$

Assuming that the wave fields vary as the real part of

$$\exp\left\{ i\left(\vec{k}.\vec{r} - \omega t + \psi_0\right)\right\}$$

we get,

$$E_z = R_e\left\{|E_z|\, e^{i(\vec{k}.\vec{r} - \omega t + \psi_0)}\right\}$$
$$= |E_z| \cos\left(\vec{k}.\vec{r} - \omega t + \psi_0\right)$$

$$E_x = R_e\left\{ C_{xz}|E_z|\, e^{i(\vec{k}.\vec{r} - \omega t + \psi_0)}\right\}$$
$$= C_{xz}|E_z| \cos\left(\vec{k}.\vec{r} - \omega t + \psi_0\right)$$

and,

$$E_y = Re\left\{ iC_{yz}|E_z|\, e^{i(\vec{k}.\vec{r} - \omega t + \psi_0)}\right\}$$
$$= -C_{yz}|E_z| \sin\left(\vec{k}.\vec{r} - \omega t + \psi_0\right) .$$

---(3.3)

With the help of equaticns (3.3), $E_\perp$, the component of the wave field E perpendicular to $\vec{B}o$ may be written as

$$E_\perp = \left(E_x^2 + E_y^2\right)^{\frac{1}{2}} = |E_z| \left\{ C_{xz}^2 \cos^2\psi + C_{yz}^2 \sin^2\psi \right\}^{1/2}$$

where $\psi = (\vec{k}.\vec{r} - \omega t + \psi_0)$ is the phase of the wave.

It is evident that the wave is elliptically polarised and $E_\perp$ varies periodcally between a minimum and a maximum. For comparison purposesit would be convenient to deal with the value of $E_\perp$ averaged over one wave period.

$$\overline{E_\perp} = \frac{2}{\pi}\int_0^{\pi/2} E_\perp \, d\psi$$

$$= \frac{2}{\pi} |E_z| \int_0^{\pi/2} d\psi \left(C_{xz}^2 \cos^2\psi + C_{yz}^2 \sin^2\psi\right)^{1/2}$$

where $\overline{E_\perp}$ is the average value of $E_\perp$.

This equation can be reduced to

$$\overline{E_\perp} = \frac{2}{\pi} C_{xz} |E_z| E\left(\frac{\pi}{2}, ecc\right)$$

where E ($\pi/2$, ecc) represents the elliptic integral of second kind and $ecc = \left(1 - \frac{C_{yz}^2}{C_{xz}}\right)^{1/2}$ is the eccentricity of the ellipse of polarisation.

Thus we finally get

$$\frac{\overline{E_\perp}}{|E_z|} = \frac{2}{\pi} C_{xz} E\left(\pi/2, ecc\right) \quad ---(3.4)$$

This expression shows that the ratio of $\overline{E_\perp}$ and $|E_z|$ is dependent on C_{xz} and C_{yz} and, therefore, it is determined both (i) by the plasma parameters like the electron plasma frequency ω_p and the electron gyro frequency Ω , and (ii) by the wave parameters like the wave frequency ω , the propagation angle θ and the total wave amplitude E, i.e. $(E_x^2 + E_y^2 + E_z^2)^{1/2}$. In majority of the cases this ratio is larger than unity which suggests that the gyro resonance effects should dominate over the Landau resonance effects.

3.2 EXTENSION OF DAS'S MODEL FOR VLF EMISSIONS:

Das's model (1968) is based primarily on the work of Kennel and Petschek (1966) although the concept involved is equivalent to quasilinear theory first developed by Vedenov et al. (1962), Engel (1965) and Andronov and Trakhtengertz (1964). However, the way in which the problem was tackled is different from them. He started with the idea that the energetic particles in the radiation belts should constitute the source of supply of energy to the VLF emissions. He considered the presence of a loss cone in the pitch angle distribution f of the trapped particles and, for simplicity, took $f = f_0$ outside and $f = 0$ inside the loss cone. He also considered existence of a back ground hiss which would grow for a distribution having a step at the loss cone angle.

For the gyroresonant particles the change in $v_{\parallel}$ in nonlinear regime is given by

$$\frac{dv_{\parallel}}{dt} = -\frac{eb}{mc} v_{\perp} \sin(\psi - \phi) \qquad \text{---(3.5)}$$

where b is the wave magnetic field and $(\psi - \phi)$ is the phase angle between $\vec{b}$ and $\vec{v}_\perp$. It has been assumed here that the propagation vector $\vec{k}$ is parallel to $\vec{B_o}$.

In a nonuniform magnetic field such as that of the earth, the $v_\parallel$ of a particle varies continuously as it moves along a field line

$$\frac{dv_\parallel}{dt} = -\frac{v_\perp^2}{2B}\frac{dB}{dz} \approx \frac{v_\perp^2}{r}$$, r being the gyroradius.

Also, the wave phase velocity $v_p = \frac{\omega}{k}$ changes as the wave moves from one point to another on the field line.

Therefore, the resonance condition for a particle is soon upset and it may go out of resonance. However, a period of effective resonance can be defined and the contributions to the change in the velocity of a particle from the resonance and from the nonuniformity of the magnetic field can be separately calculated and compared.

The effects of resonance will be substantial and worth consideration only if the change in $v_\parallel$ due to

the resonance is large compared to that due to the nonuniformity of the field over the period of effective resonance. This condition can be mathematically put as (Das, 1968)

$$\frac{eb}{mc} \sin\psi > \frac{v_\perp}{r}$$

where r is the radius of gyration of a particle.

This condition is strictly true at the equator and it is not satisfied at points far away from the equator. It shows that the resonant effects in the earth's geomagnetic field would be strong and important only in the equatorial region. Incidentally, observations of VLF emissions also show that they are generated near the equator and thereby suggest that the resonant interaction night have something to do with the emissions.

A wave packet would resonate with particles over a finite range of velocities owing to the finite width of its spectrum. The whole of the velocity space can be divided into two parts (see fig.3.1): resonant and nonresonant. The nonresonant region can be taken as

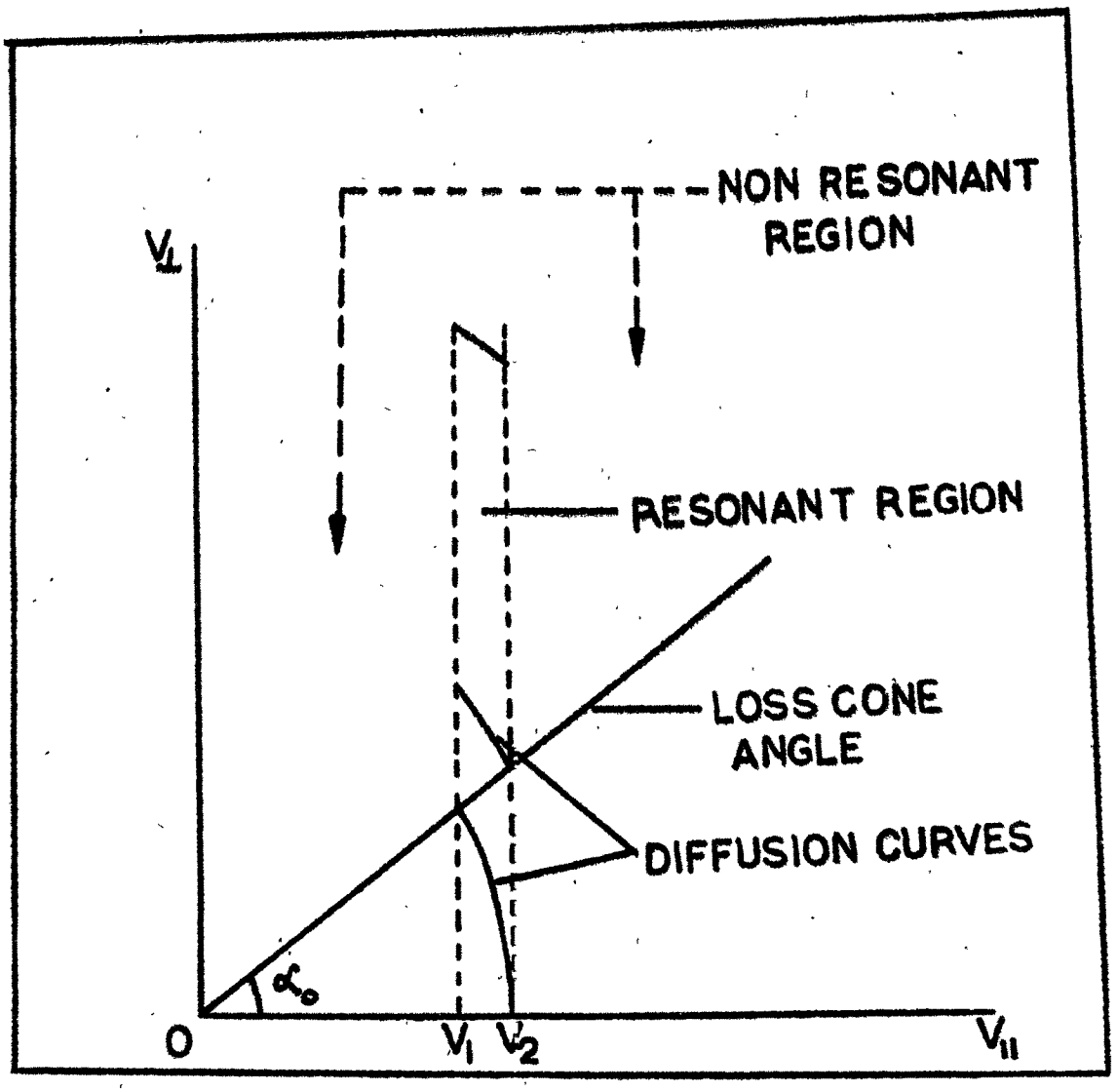

FIGURE 3.1

THE RESONANT AND NONRESONANT REGIONS IN VELOCITY SPACE. THE PARTICLES DIFFUSE ALONG DIFFUSION CURVES THROUGH RESONANCES.

unaffected by the waves and the distribution function therein may be assumed to remain unchanged with time. In the resonant region, the particles, will be trapped and the eddies will be formed in the phase space. The trapping period T is given by

$$\frac{2\pi}{T} = \frac{e}{mc}\left(Bb \tan\alpha\right)^{1/2}$$

For $b \sim 1$ m and $L \sim 3$, T comes out to be about 0.1 sec. If a particle remains in a wave packet for a time much larger than T, each eddy will take many turns and the final distribution f along each eddy will be constant. The process is similar to diffusion in velocity space where the particles are constrained to move along certain diffusion curves. It can be shown that f will become constant along these diffusion curves and $\frac{\partial f}{\partial v_{\parallel}}$ will become highly negative at the boundaries of the resonant region but at the central resonant $v_{\parallel}$ it will become zero. The growth rate γ for such a system is given by following equation (Vedenov et al. 1962)

$$\gamma = -\frac{\pi k^2 v_{res}^2}{n\Omega}\int_0^\infty \left[v_\perp \frac{\partial f}{\partial v_\parallel} - (v_\parallel - v_p)\frac{\partial f}{\partial v_\perp}\right]_{v_\parallel = v_{res}} v_\perp^2 \, dv_\perp \qquad (3.6)$$

where n is electron concentration and v_{res} is the gyroresonant $v_\parallel$.

It can be shown that $\int_{-\infty}^{\infty} \gamma \, dv_\parallel$ is a constant. Since γ, in the nonresonant region, does not change with time and that in the resonant region is reduced with time because of the redistribution of the particles, it can be inferred that large peaks in γ will occur near the boundaries of the disturbed region.

If the particle remains in the wavepacket for a time much shorter than the trapping period T, the linear theory can be applied to study its motion. The resonant particles situated near the loss cone boundary are redistributed in such a fashion that the loss cone boundary in its modified form looks like a conical screw (see fig. 3.2). When the wave packet has passed, the fine structure is smeared out and the new distribution thus developed is found to give high growth rates

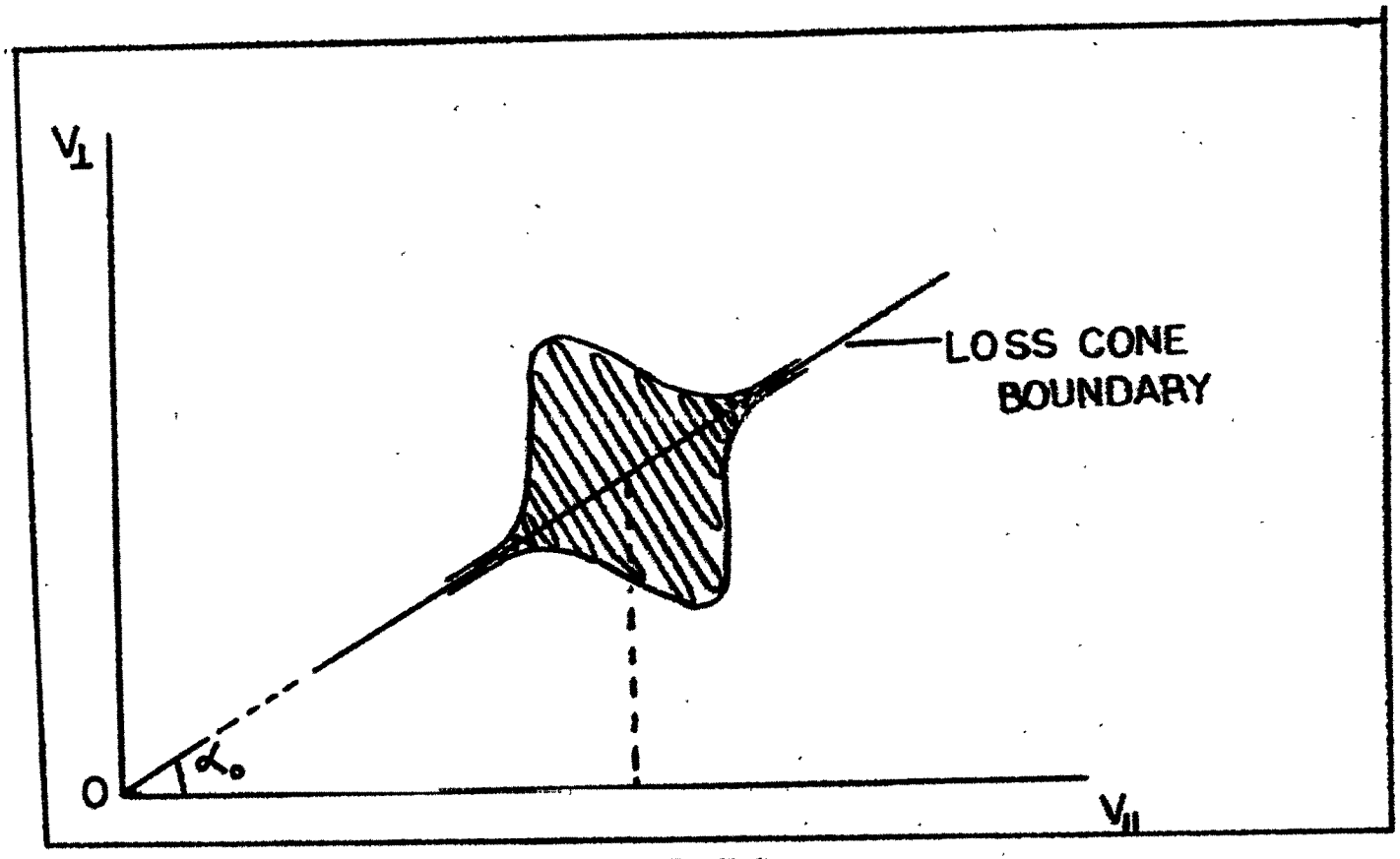

FIGURE 3.2

THE GYRORESONANCE OF A PULSE DISTORTS THE DISTRIBUTION AT LOSS CONE BOUNDARY. THE DISTURBANCE TAKES THE FORM OF A CONICAL SCREW.

at frequencies resonant with slightly higher and slightly lower $v_{\parallel}$ than the central resonant $v_{\parallel}$ for the wave packet (Das, 1968).

Fig. (3.3) shows the region in the velocity space where the distribution function is modified.

The figure shows two gaussian curves symmetrically situated on either side of the loss cone angle α_0 in $v_{\parallel} - v_{\perp}$ space. Before the interaction the distribution function is $f = f_0$ for $\alpha > \alpha_0$ and $f = 0$ for $\alpha \leq \alpha_0$. However, after the wave-packet has passed, the distribution gets modified in the region bounded by the two gaussians while it still remains equal to f_0 above the upper gaussian and equal to zero below the lower gaussian. In the disturbed region, f increases from zero at the lower gaussian as we move upwards and finally becomes f_0 when we reach the upper gaussian. If we draw a straight line perpendicular to the loss cone at Q $(v_{\parallel}', v_{\perp}')$ which intersects upper gaussian at R $(v_{\parallel}'', v_{\perp}'')$ and the lower gaussian at S $(v_{\parallel}''', v_{\perp}''')$ as shown in the figure, then the distribution f at a point P $(v_{\parallel}, v_{\perp})$ on the line would be given by

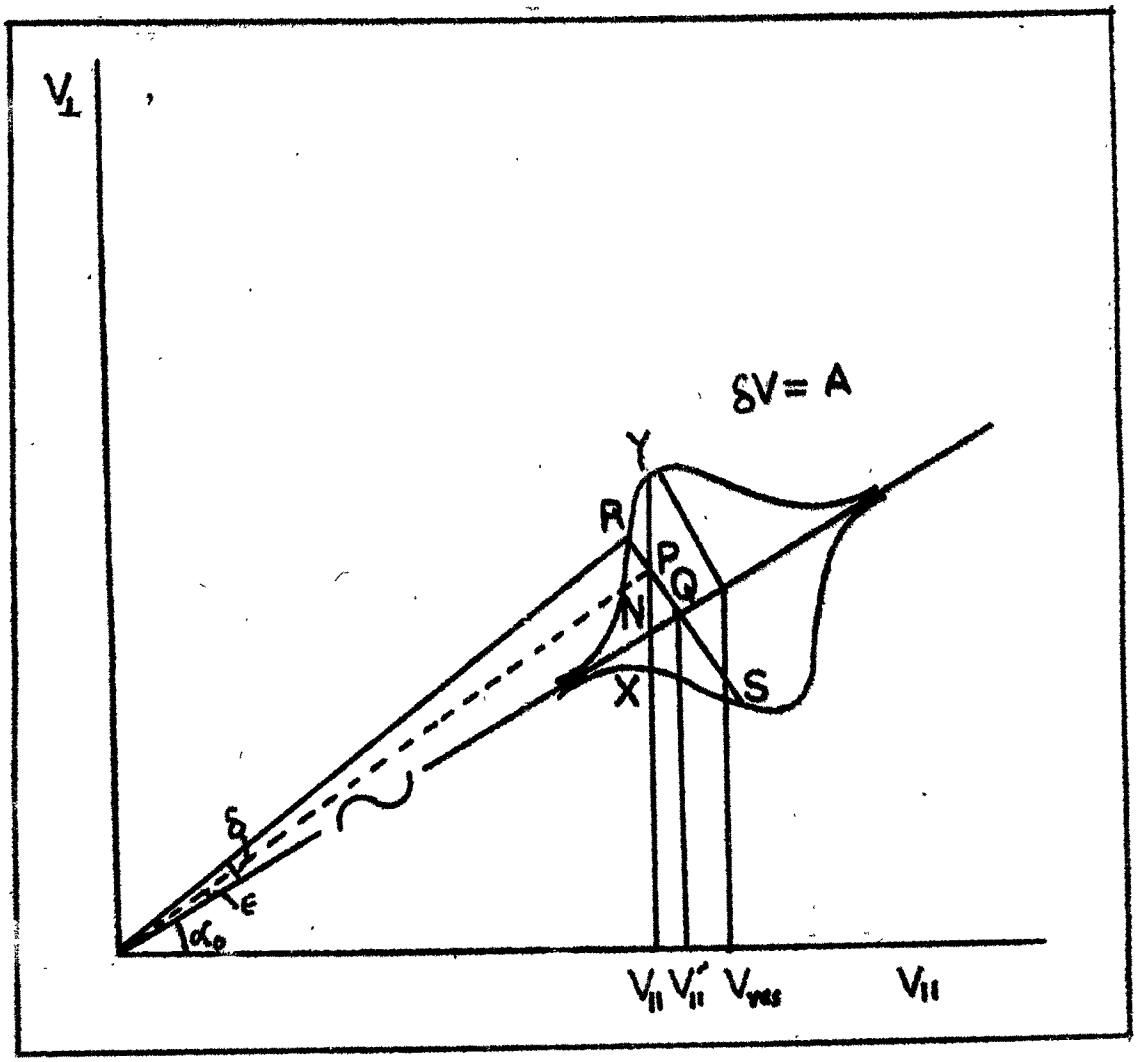

FIGURE 3.3

DISTRIBUTION GETS MODIFIED IN THE REGION BOUNDED BY THE TWO GAUSSIANS. THE COORDINATES OF P, Q, R AND S ARE RESPSCTIVELY ($V_{||}$, $V_\perp$), ($V_{||}'$, $V_\perp'$), ($V_{||}''$, $V_\perp''$) AND ($V_{||}'''$, $V_\perp'''$)

$$f = \frac{1}{2} f_0(v_\perp'' / v_\perp)\left[1 + \frac{2}{\pi} \sin^{-1}\left(\frac{\epsilon}{\delta}\right)\right] \quad \text{---} \quad (3.7)$$

where ϵ = $\angle$ POQ and δ = $\angle$ ROQ. The growth rate for such a distribution function would be given by

$$\gamma = \int \frac{1}{2} f_0 \, v_\perp'' \, v_\parallel' \sec\alpha_0 \left[\frac{2}{\pi} \frac{v_\perp / \delta v}{\pi[1-(\epsilon/\delta)^2]^{1/2}} - \left\{1 + \frac{2}{\pi} \sin^{-1}\left(\frac{\epsilon}{\delta}\right)\right\} \cos\alpha_0\right]$$

$$\text{---} \quad (3.8)$$

where the integration for the growth rate at frequency ω has to be carried out from the point of intersection X of the straight line $v_\parallel = \frac{|\omega - \Omega|}{k}$ with the lower gaussian to the point of intersection Y of the same straight line with the upper gaussian.

The various relationships between the co-ordinates of P,Q,R and S and the angles α and δ are listed below:

$$v_{\perp}'' = v_{11} \tan\alpha_0 + \delta v \sec\alpha_0$$

$$v_{11}' = v_{11} + \delta v \sin\alpha_0$$

$$\epsilon = v_{\perp}\cos\alpha_0 - v_{11}\sin\alpha_0$$

where $\delta v = v_{11}\sec\alpha_0 . \delta$

$= A \exp\{-(v_{11}-v_{110})^2 \sec^2\alpha_0/d^2\}$. The last equation determines the form of the envelope of the wave packet such that A and d represent the amplitude and the band width of the wave packet and consequently the dimensions of the disturbed region. v_{110} is the value of v_{11} of the particles which resonate with the central frequency of the wave packet.

The results obtained from the model are very interesting. The growth rate is reduced at the central frequency while enhancements occur at two frequencies slightly above and below the central frequency (see fig.3.4).

The peaks in the growth rate suggest that the waves inside the wave packet at corresponding frequencies

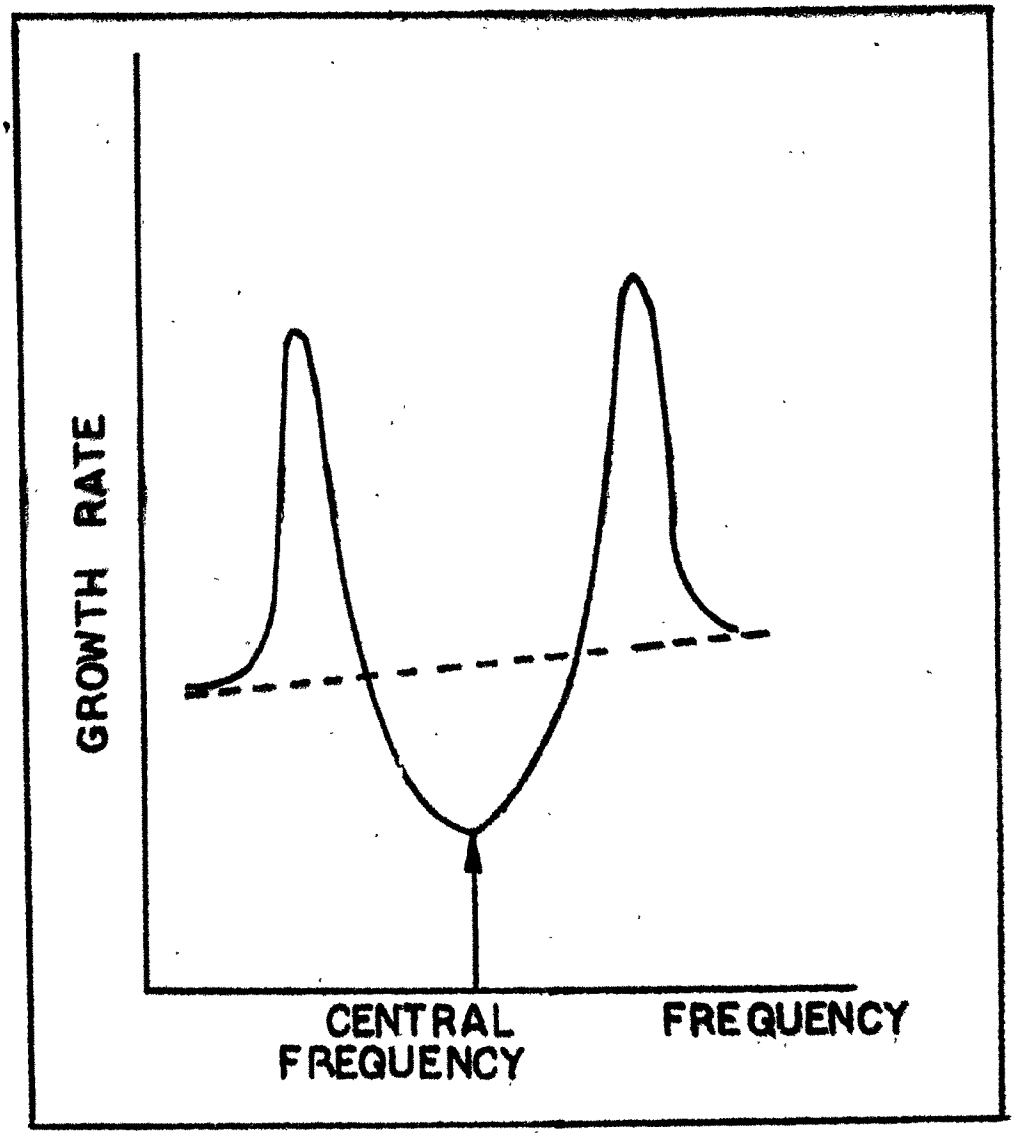

FIGURE 3.4

A TYPICAL GROWTH RATE VERSUS FREQUENCY CURVE FOR A PERTURBATION MOVING THROUGH THE MODIFIED DISTRIBUTION OF PARTICLES

shall grow and are likely to be observed as emissions. This furnishes a mechanism for the generation of VLF emissions.

The amplification is essentially due to resonant interaction between the whistler mode wave packet and the energetic particles of the medium. The amplitude of the wave packet ~~and~~ in the previous model is restricted to a critical value to avoid complications in the computational procedure. However, the increase in amplitude beyond the critical value brings into picture two distinct regions in the velocity space contributing to the growth of the waves at the same frequency. It would be interesting to study the behaviour of the growth rate for amplitudes of the wave packet larger than the critical one and compare it with the growth rates obtained from smaller amplitude pulses. In what follows, the details of the computation of growth rate and a suitable computer programme evolved for the purpose have been discussed.

The extended model for the localised disturbed region in velocity space is shown in fig. (3.5). The disturbed region for the small amplitude wave discussed

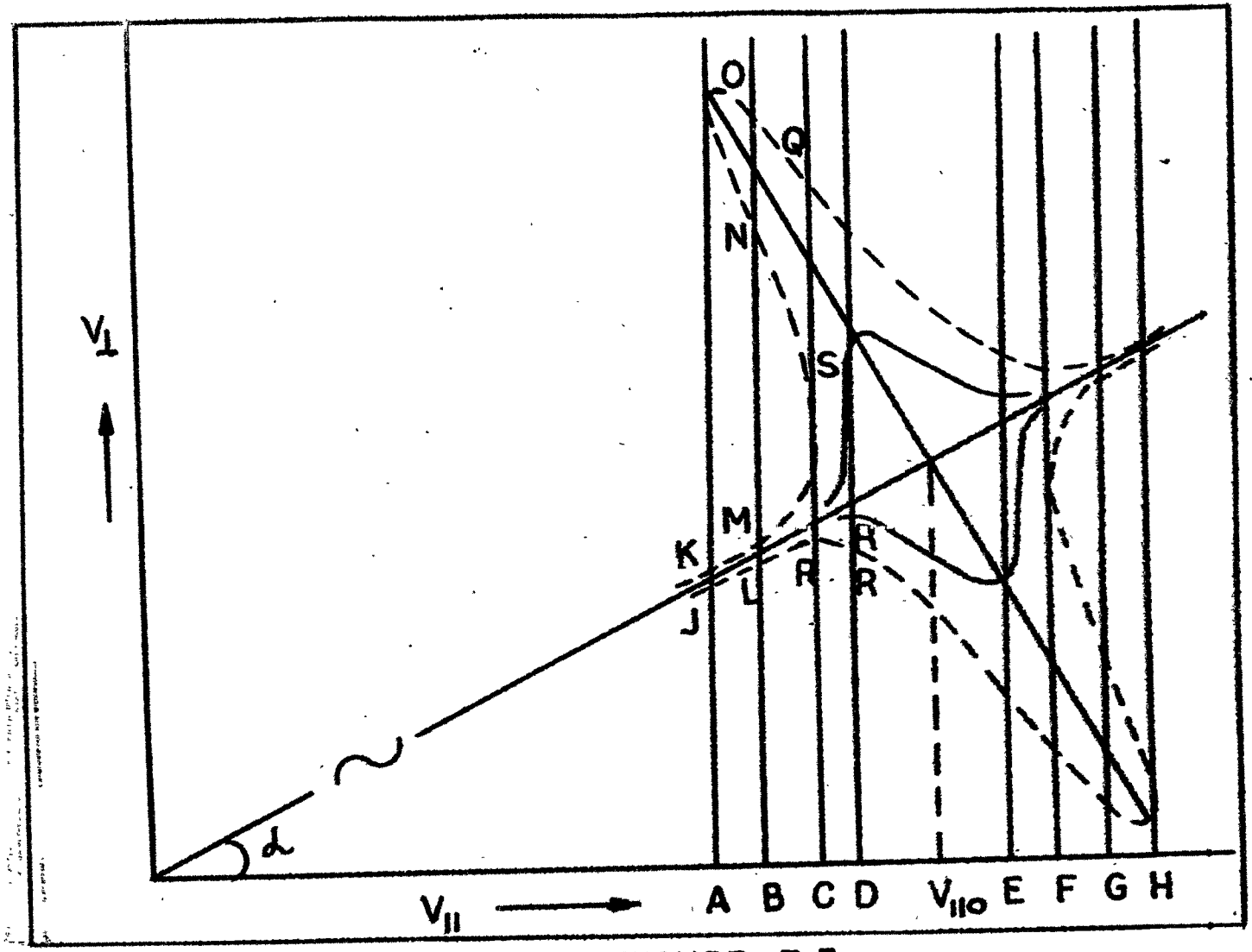

FIGURE 3.5

COMPARISON OF DISTURBED REGIONS DUE TO SMALL AND LARGE AMPLITUDE PULSES.

in the previous model is shown to be bounded by continuous solid Gaussian curves and that for the large amplitude wave considered here has been shown to be bounded by the dashed gaussian curves. The difference between the previous situation and the present one arises from the fact that we meet the disturbed region only once in the previous situation and sometime once and some times twice in the present situation as we move from the lower gaussian to the upper gaussian in the disturbed region along the straight line $v_{11} = |v_{11G}| = |v_{res}| = \frac{|\omega - \Omega|}{k}$. This situation arises only for those gaussian boundaries whose amplitude exceeds a certain critical limit A_c given by

$$A_c = \frac{e\alpha^{1/2}}{2 \tan \alpha_0} \qquad \text{---} \quad (3.9)$$

If the amplitude A of the wave packet is less than A_c, it can be handled by the computation procedure developed for the earlier model. However, for $A > A_c$ that will not be sufficient unless suitably modified.

The contribution to the growth rate in this case at B (see fig.3.5) comes from the region L to M

as well as from N to O . Similar things happen at any $v_{\parallel}$ lying between OA and OC and between OF and OH. The $v_{\parallel}$'s lying between OC and OF do not show this peculiar behaviour. We presume that the growth rate given by equation (8) still holds good. However, we have to calculate it separately for the two regions that contribute to it and then to add up them together.

The limits of integration are obtained by finding the points of intersection of a straight line parallel to $v_{\perp}$ axis with the gaussian boundaries of the disturbed region.

The growth rate computations for wavepackets with amplitudes less than the critical amplitude is easy because the line along which the integration is to be carried out does not intersect one gaussian at more than one points. For example, at $v_{\parallel}$ = OD , the integration is to be carried out only from R to S.

The problem of integration for computing the growth rate for a large amplitude pulse shown by the dashed curves in figure (3.5) is complicated because a vertical line at some values of $v_{\parallel}$ intersects

one of the gaussians at more than one points. The integration procedure for $OH < v_{\parallel} < OA$ and $OC < v_{\parallel} < OF$ remains the same while for values of $v_{\parallel}$ between OA and OC and between OF and OH, the integration has to be carried out separately for different ranges in the disturbed region at the same value of $v_{\parallel}$, e.g., at $v_{\parallel} = OB$, the integration has to be carried out from L to M and then from N to O.

Thus it is necessary to determine the limits of integration by solving the equation of the gaussian and that of the vertical line at $v_{\parallel}$ under question simultaneously. The computer programme is divided into two parts, the first part being for those values of $v_{\parallel}$ where the vertical line intersects each curve only at one point, and the second part for those values of $v_{\parallel}$ where the vertical line intersects one of the curves at three points and the remaining curve at one point only.

The method of false position was used to determine the exact points of intersection which is slightly complicated in the second part. After the

limits are obtained, the integration is performed in the following way. The distance between the limits of integration is divided into 25 equal steps. The integrand is calculated at the centre point of each step and is then multiplied by the length of the step. The total value of the integral is given by adding up all the contributions from different steps. In the region where the integration is to be carried out for two different sets of limits at same $v_{\parallel}$, the individual contributions are added up to give the total value of the growth rate at the given value of $v_{\parallel}$.

3.3 RESULTS AND DISCUSSION:

The results obtained are shown in fig.(3.6). The continuous curve represents the growth rate at different resonant $v_{\parallel}$'s in the case of a disturbing pulse having its amplitude less than the critical amplitude A_c . The dashed curve describes the growth rate in the case when amplitude of the disturbing

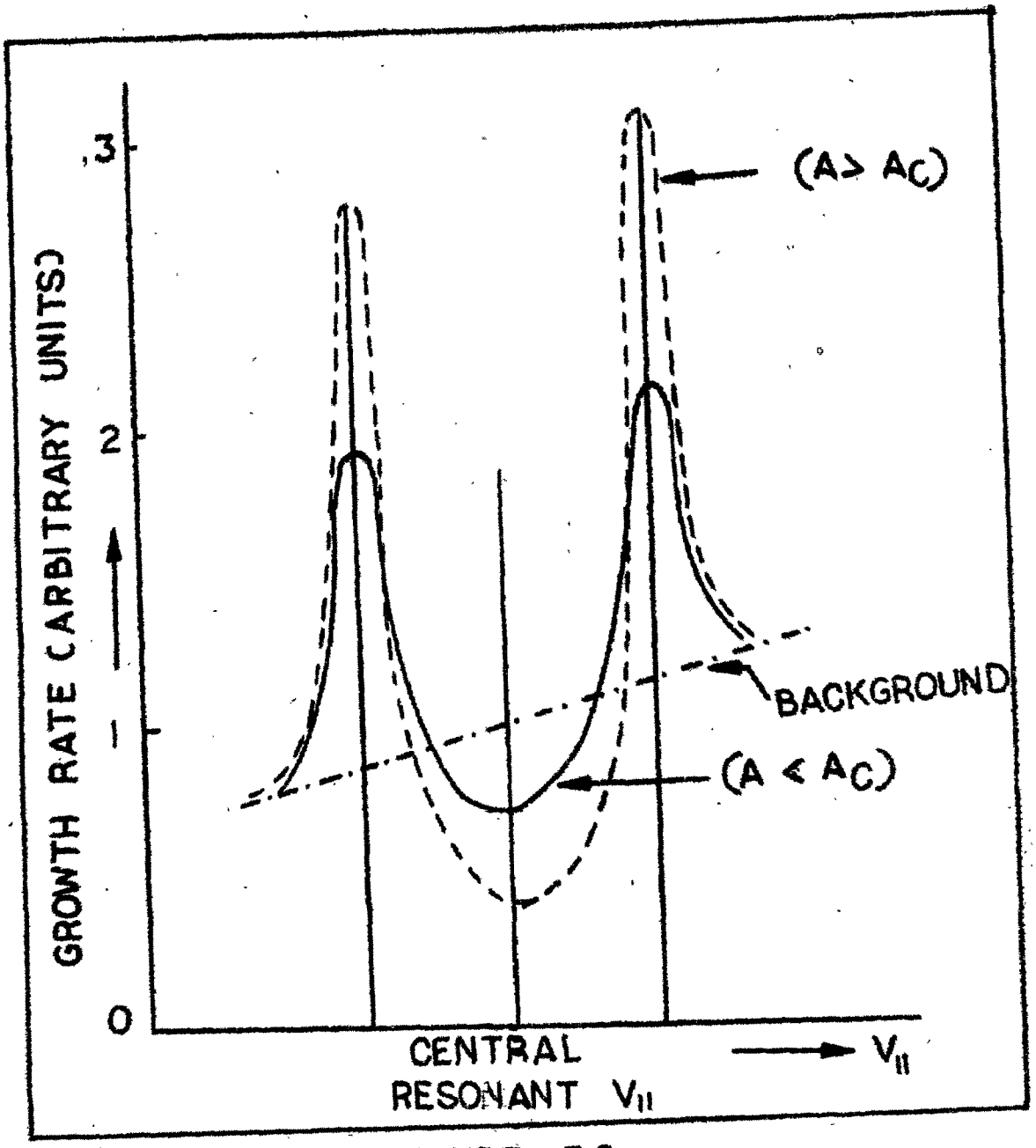

FIGURE 3.6

COMPARISON OF GROWTH RATES OBTAINED FROM THE DISTRIBUTION DISTURBED BY THE LARGE AND THE SMALL AMPLITUDE PULSES.

pulse is large compared to the critical amplitude A_c. In both cases it is seen that the growth rate is reduced at the central frequency range while enhancements occur at the frequencies slightly above and below the central frequency. In order that proper comparisons can be made of the results obtained from the previous and the extended models, care is taken to vary the amplitude A and the width d of the wave-packet in such a way that $\int |A(v_{\parallel}, \text{sech}\,\ell)|^2 \, dv_{\parallel}$ remains the same. This amounts to saying that, as we go on increasing the amplitude, we go on decreasing the frequency width of the pulse, or equivalently saying, we go on increasing the duration of the pulse keeping the energy content of the pulse constant.

As figure (3.6) shows, the growth rate of the sidebands of the wave packet is much larger for the extended model when compared with the same for the earlier model (Das and Vyas, 1971).

This sudden change occuring at the critical amplitude (which will correspond to a critical time duration of the pulse) should account for the frequent triggering of VLF emissions by Morse code dashes

(duration 150 ms) and fewer triggerings by Morse code dots (duration 50 ms). The effect is probably because of the sudden appearance of two regions contributing to the growth at the same frequency.

Tantry (1970) has recently reported that he has frequently observed duplicate traces of whistlers at a time difference of 15 msec. It is interesting to mention here that the computation of the time lag of perturbations corresponding to these two peaks in the growth rate, to be observed at a ground station in the model shows a difference of the order of 20 msec. Therefore, if these traces are treated as emissions, the model described here is quite adequate to explain these observations.

The critical amplitude A_c is a function of the bandwidth d (see eq.3.9) and it increases with increase in d. This shows that the critical amplitude will be large for small duration pulses. A pulse should have its amplitude greater than the critical amplitude so as to give large growth rates and therefore, if it has also a large band width, it must have its total energy content, $\int |E(\omega)|^2 d\omega$,

large enough to attain this critical amplitude at its central frequency. (Here E(ω) is the wave amplitude at the frequency ω inside the pulse). We can, in general say that short duration pulses like the Morse code dots are also capable of triggering emissions, if they are sufficiently strong to have their amplitude greater than A_c. This explains how some times dots have also been able to trigger VLF emissions.

Another interesting result was obtained when the growth rate calculations were extended to those pulses for which the amplitude A was much large compared to A_c. It was found that secondary peaks were protruding above the background.. However, the growth rates corresponding to these peaks were not large compared to background growthrate. Therefore, it was decided to consider strong pulses with large bandwidth and large amplitude ($A >> A_c$) and the results obtained are as shown in fig. (3.7). Two peaks in the growth rate appear on each side of the central

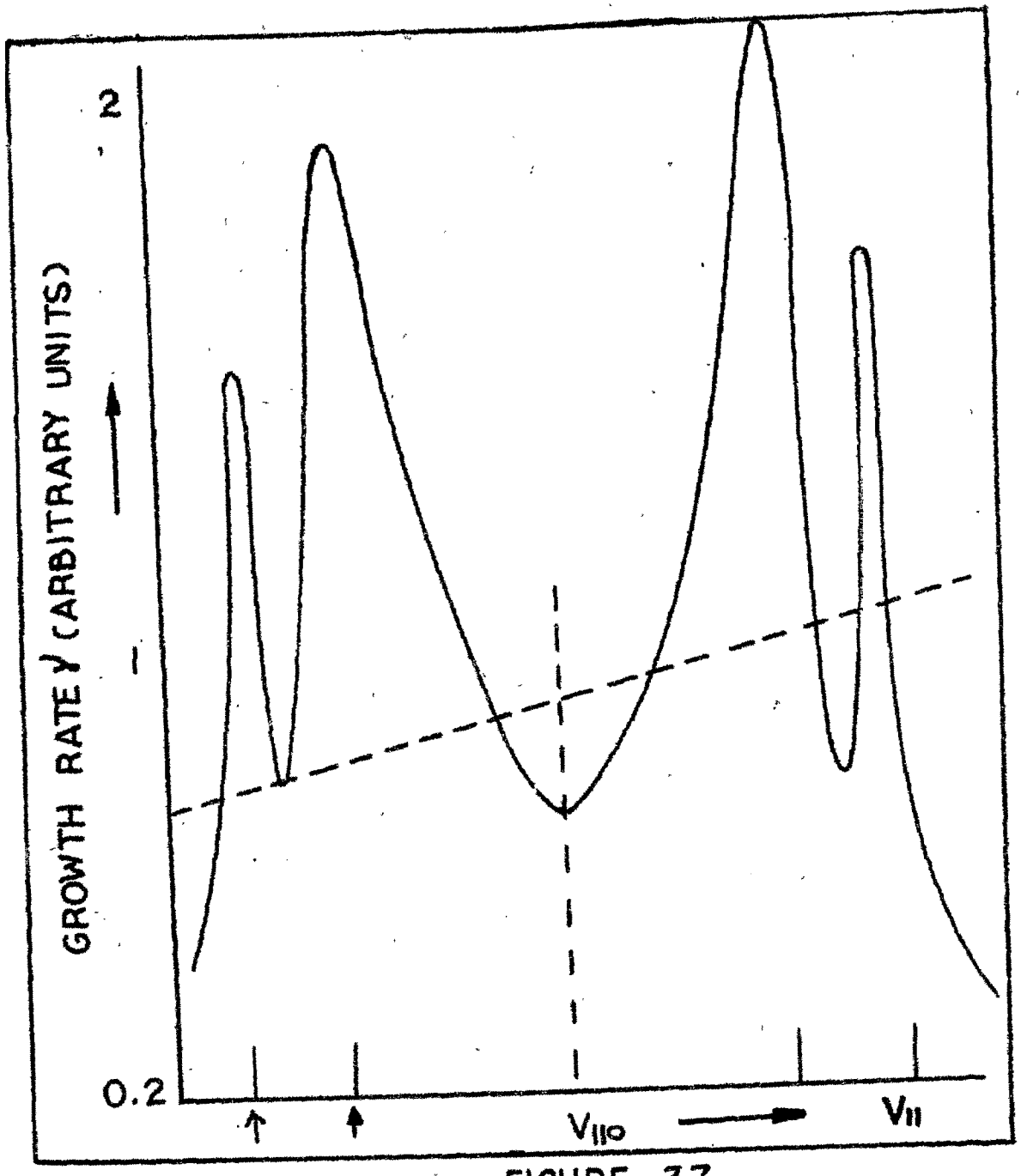

FIGURE 3.7

GROWTH RATE γ VERSUS V_{11}

CONTINUOUS CURVE : γ FOR DISTURBED DISTRIBUTION

BROKEN CURVE : γ FOR UNDISTURBED DISTRIBUTION

(CASE OF A STRONG BROAD BAND PULSE)

frequency instead of one seen in fig.(3.6). The growth rate at central frequency is reduced as before. This shows that a very strong wavepacket is capable of producing multiple emissions also.